

The Sessile Drop as a Heterogeneous Nucleation Embryo

by
W. R. Barchet

Technical Paper No. 123
Department of Atmospheric Science
Colorado State University
Fort Collins, Colorado



**Department of
Atmospheric Science**

Paper No. 123

THE SESSILE DROP AS A
HETEROGENEOUS NUCLEATION EMBRYO

by

William Richard Barchet

This report was prepared with support from
the National Science Foundation
Grant No. GA-930
Principal Investigator, Myron L. Corrin

Department of Atmospheric Science
Colorado State University
Fort Collins, Colorado

June 1968

Atmospheric Science Paper No. 123

ABSTRACT

Basic thermodynamic concepts are applied to the condensation of a vapor resulting in a general expression for the free energy change of the system for the formation of a nucleation embryo. No assumptions about the geometry of the embryo are made. Spherical approximation of the shape of the embryo leads to the usual free energy change expressions.

A nonspherical embryo, the sessile drop, is investigated as a nucleation embryo. The surface areas and volume of the sessile drop are developed for use in the free energy change equation and are found to reduce to those of a spherical cap for limiting conditions of size, contact angle, and gravitational effect.

Numerical computations of the free energy change for a sessile drop shaped embryo are made for water and for mercury. These computations demonstrate that the spherical cap approximation adequately describes the free energy change for the formation of an embryo shaped as a sessile drop.

William Richard Barchet
Atmospheric Science Department
Colorado State University
Fort Collins, Colorado 80521
June, 1968

ACKNOWLEDGEMENTS

The author wishes to express his appreciation for the guidance and encouragement given him by his adviser, Dr. M. L. Corrin, during the months of work involved in this paper. The financial support given to the author for the past two years by the University Corporation for Atmospheric Research is gratefully acknowledged. Mrs. Janice Piper is to be commended and thanked for typing this manuscript under a tight time schedule.

This research was sponsored by the National Science Foundation under Contract GA-930.

This material is based upon a thesis submitted as partial fulfillment of the requirements for the Master of Science Degree at Colorado State University.

TABLE OF CONTENTS

	Page
TITLE PAGE	i
ABSTRACT	ii
ACKNOWLEDGEMENTS	iii
LIST OF TABLES	vi
LIST OF FIGURES	vii
INTRODUCTION	1
THE THERMODYNAMICS OF NUCLEATION	5
Generalized Thermodynamics of Nucleation	5
Homogeneous Nucleation	12
Heterogeneous Nucleation	13
SPHERICAL APPROXIMATION OF THE EMBRYO SHAPE	15
Homogeneous Nucleation	15
Heterogeneous Nucleation	16
Nonspherical Shapes	17
THE SESSILE DROP	19
THE SESSILE DROP AS AN EMBRYO	26
NUMERICAL COMPUTATIONS	32
CONCLUDING REMARKS	46
BIBLIOGRAPHY	51

TABLE OF CONTENTS - Continued

	Page
APPENDIX I. SERIES SOLUTIONS FOR SESSILE DROP SHAPE	53
APPENDIX II. COMPUTER PROGRAM	56
APPENDIX III. TABULATED DATA	58

LIST OF TABLES

Table		Page
1	Input data	59
2	The error and relative error as a function of \underline{X} . .	60
3	Dependence of the relative error on the supersaturation.	61
4	Dependence of the relative error on the contact angle	62

LIST OF FIGURES

Figure		Page
1	The spherical cap heterogeneous nucleation embryo	16
2	The sessile drop	20
3	The error in assuming $\Delta G_{\text{sessile drop}}$ is given by $\Delta G_{\text{spherical cap}}$ for 0.1 percent supersaturation and a contact angle of 34.4 degrees as a function of \underline{X}	37
4	The relative error in assuming $\Delta G_{\text{sessile drop}}$ is given by $\Delta G_{\text{spherical cap}}$ for 0.1 percent supersaturation and a contact angle of 34.4 degrees as a function of \underline{X}	38
5	The maximum relative error as a function of the supersaturation at a contact angle of 34.4 degrees . .	39
6	The relative error at the critical radius as a function of the supersaturation at a contact angle of 34.4 degrees	40
7	The maximum relative error as a function of contact angle for a supersaturation of 0.1 percent	41
8	The relative error at the critical radius as a function of contact angle for a supersaturation of 0.1 percent	42
9	The relative error for mercury compared to water at a supersaturation of 0.1 percent and contact angle of 34.4 degrees as a function of \underline{X}	43
10	The maximum relative error for mercury compared to that for water as a function of supersaturation at a contact angle of 34.4 degrees	44

LIST OF FIGURES - Continued

Figure		Page
11	The maximum relative error for mercury compared to that for water as a function of contact angle at a supersaturation of 0.1 percent	45
12	The error in assuming $\Delta G_{\text{sessile drop}}$ is given by $\Delta G_{\text{spherical cap}}$ for the hypothetical case as a function of \underline{X}	49
13	The relative error for the hypothetical case as a function of \underline{X}	50
14	The computer program for computing the free energy change	57

INTRODUCTION

The phenomena of phase changes can be examined from several view points. Using statistical mechanics and molecular models, the physical mechanism of each step in a phase change can be theoretically described. A more general approach is to apply basic thermodynamic concepts to changes of phase. With the thermodynamic approach only the initial and final states of the system are of importance. The actual physical mechanism of the change of the system is avoided in the thermodynamics. Using the basic principles presented by Gibbs (1906) and by Frenkel (1946) it is possible to derive an equation which describes the formation of the condensed phase in terms of the free energy change of the system. A particular feature of this derivation is that no assumption about the geometry of the condensed phase is necessary to obtain the free energy change expression. Mason (1957) and Fletcher (1962) present similar derivations of the free energy change for the system except that they assume the embryo of the condensed phase is spherical.

The derivation of the free energy change of the system for the formation of an embryo of the condensed phase leads to the question about the effect of nonspherical shapes on the free energy change. The work of Bashforth and Adams (1883) on the shape of the

sessile drop is extended to provide information on the surface areas and volume of the sessile drop. Using this information the effect of a nonspherical embryo shape on the free energy change is compared to the free energy change using a spherical embryo for water and for mercury systems.

For the convenience of the reader the definitions of the symbols used in the text are given below. Where several definitions are used for the same symbol, the definitions are given in the order of occurrence in the text. Also, the page number on which the symbol first appears is given to the right of the definition. The context in which such symbols are used thereafter should make the definition which applies obvious.

A - Surface area (6)

ΔA - Change in surface area (6)

A_c - Surface area correction term (27)

b - Radius of curvature at the vertex (21)

β - Shape parameter for the sessile drop (21)

d - 1) Differential operator (8)

2) Density of sessile drop (20)

Δ - 1) Finite differential operator (7)

2) Absolute error (27)

δ - 1) Variation differential operator (10)

2) Relative error (28)

- δ - Partial differential operator (6)
- G - Free energy (6)
- ΔG - Change in free energy (7)
- ΔG^* - Critical free energy change (17)
- g - 1) Number of molecules in embryo (5)
2) Acceleration of gravity (20)
- i - Summation index (6)
- M - Gram-molar weight of a substance (31)
- m - Number of moles of a substance (8)
- N - Number of molecules in the system (5)
- n - Number of molecules (6)
- p - Vapor pressure (6)
- p_{∞} - Reference vapor pressure (9)
- ϕ - Angle parameter (19)
- R - 1) Universal molar gas constant (9)
2) Principal radius of curvature (20)
- r - Radius (15)
- r^* - Critical radius (15)
- ρ - Meridional radius of curvature (20)
- L, V - Subscripts denoting the liquid-vapor interface (12)
- S, L - Subscripts denoting the solid-liquid interface (13)
- S, V - Subscripts denoting the solid-vapor interface (13)
- Σ_i - Summation over values of \underline{i} (7)
- σ_i - Surface free energy of the \underline{i} -th interface (6)

- T - Temperature (6)
- θ - Contact Angle (13)
- μ° - Standard state chemical potential (9)
- μ_e - Chemical potential of a substance in the condensed phase (7)
- μ_v - Chemical potential of a substance in the vapor phase (7)
- V - Volume (8)
- V_c - Volume correction term (27)
- ΔV - Change in volume (8)
- V_m, \bar{V} - Molar volume (8)
- ΔV^* - Critical volume change (11)
- x - 1) Horizontal coordinate (19)
- 2) Radius of embryo compared to critical radius (27)
- z - Vertical coordinate (20)

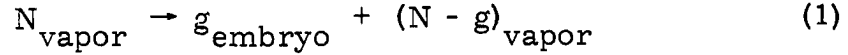
THE THERMODYNAMICS OF NUCLEATION

A physical description of the process by which a vapor condenses was given by Frenkel (1939) as an increase in the number and size of heterophase fluctuations within the vapor. A heterophase fluctuation in the vapor is an aggregation of molecules forming a small cluster, an embryo, resembling the condensed phase. When the temperature and pressure of the vapor approach the condition for condensation the number and size of these embryos increase. In a discussion of the thermodynamics of this process, the physical mechanism by which molecules collide and aggregate to form clusters is not of interest or importance. The system to which the following discussion applies contains molecules of one substance in the vapor state and in one embryo. The thermodynamics of nucleation within this system is concerned only with the initial and final states of the system.

Generalized Thermodynamics of Nucleation

The system to be examined is a volume initially containing N molecules of one chemical substance as a vapor at a constant temperature and pressure. The total pressure on the system is the pressure of the vapor. By some unspecified process g molecules aggregate to form a single embryo within the

volume. The final state of the system is $(N-g)$ molecules in the vapor phase and g molecules in the embryo, the condensed phase. This change of the system can be schematically written as



where the subscripts refer to the phase in which the molecules are found. The relative probability that the system will undergo such a change is determined by the free energy change of the system.

For a one component system the free energy per molecule in the vapor is given by the chemical potential of the substance in the system. The chemical potential of a substance in a one component system is defined as

$$\mu = \left(\frac{\partial G}{\partial n} \right)_{T, p, A} .$$

The subscripts refer to quantities that are held constant during the differentiation. The free energy of the embryo is given by the sum of the bulk free energy of the substance in the embryo and the free energy due to the surface areas of the embryo. The bulk free energy is given by the product of the chemical potential and the amount of substance in the condensed phase. A surface free energy represents the work required to form an interface between two phases and is defined as

$$\sigma_i = \left(\frac{\partial G}{\partial A_i} \right)_{T, p, A_{j \neq i}}$$

for a one component system. The subscript \underline{i} is used to allow for more than one interface and surface free energy to be associated with the embryo. The total free energy of the embryo is then

$$\mu_e g + \sum_i \sigma_i \Delta A_i \quad (2)$$

where μ_e is the chemical potential of the substance in the condensed phase. If more than one interface is present, the summation is over the total number of interfaces and ΔA_i is the change in surface area of the \underline{i} -th interface having a surface free energy of σ_i . With these definitions the free energy change of the system from the initial to final state can be written as

$$\Delta G = (\mu_e - \mu_v) g + \sum_i \sigma_i \Delta A_i . \quad (3)$$

The chemical potentials, as used in equation 3, are given on a per molecule basis. However, since thermodynamics is designed to deal only with macroscopic systems, the concept of molecules is irrelevant. Much discussion has been lavished on the problem of extending thermodynamics to deal with these microscopic systems by assuming the microscopic system has the properties of similar macroscopic systems. Stating that a cluster of \underline{g} molecules has a surface energy equivalent to a macroscopic drop immediately raises the question of how many molecules are necessary to constitute a new phase. It is difficult to assume that a cluster of three or four molecules has a surface free energy equal to that for the

condensed phase. This problem is avoided here by assuming that the final state of the system is such that the embryo is large enough to possess macroscopic properties. As stated by Guggenheim (1949), the embryo is assumed to constitute a condensed phase. Since thermodynamics deals only with the end states, the physical process of changing the system from one state to another does not enter the picture. Conclusions based on the thermodynamics must be made with the nature of this assumption in mind.

The molecular concept can be abandoned in favor of molar quantities. Now the chemical potentials are given for one mole of substance and \underline{g} is replaced by the volume change of the embryo divided by the molar volume of the condensed phase. The free energy change expression becomes

$$\Delta G = (\mu_e - \mu_v) \frac{\Delta V}{V_m} + \sum_i \sigma_i \Delta A_i . \quad (4)$$

Changes in volume and surface area of the embryo are used to represent the volume and surface areas so that growth of an embryo can be discussed later in the paper. In the process of formation of an embryo there is no difference between these two statements of the volume and surface areas.

The differential change in free energy at constant temperature of a single component phase is

$$dG = VdP + \mu dm$$

where \underline{m} is the number of moles of the substance. The differential \underline{dG} is exact; therefore, cross-differentiation of the right-hand terms yields

$$\left(\frac{\partial \mu}{\partial p}\right)_{T, m} = \left(\frac{\partial V}{\partial m}\right)_{T, p} = \frac{V}{m} = \bar{V} \quad (5)$$

where \bar{V} is the molar volume of the substance. Considering the vapor to behave as an ideal gas, equation 5 becomes

$$\left(\frac{\partial \mu}{\partial p}\right)_{T, m} = \frac{RT}{p}$$

or
$$d\mu = RT \frac{dp}{p} \quad (6)$$

Integrating equation 6 gives

$$\mu = RT \ln p + \mu^\circ$$

where $\underline{\mu}^\circ$ is an arbitrary constant evaluated at some standard pressure. Using this definition, the chemical potential of the substance in the embryo is

$$\mu_e = RT \ln p_\infty + \mu^\circ \quad (7)$$

where \underline{p}_∞ is the vapor pressure of the condensed phase in equilibrium with its vapor, i. e., over a plane surface. The chemical potential $\underline{\mu}_v$ is given by the vapor pressure on the system, thus

$$\mu_v = RT \ln p + \mu^\circ \quad (8)$$

The difference between the chemical potentials defined in equations 7 and 8 is

$$\mu_e - \mu_v = -RT \ln(p/p_\infty). \quad (9)$$

If the embryo-vapor system is considered to be in equilibrium with regard to a change in volume of the embryo, a volume variation of the free energy change yields

$$\frac{\delta(\Delta G)}{\delta(\Delta V)} = (\mu_e - \mu_v) \frac{1}{V_m} + \sum_i \sigma_i \frac{\delta(\Delta A_i)}{\delta(\Delta V)} = 0 \quad (10)$$

or

$$\mu_e - \mu_v = -V_m \sum_i \sigma_i \frac{\delta(\Delta A_i)}{\delta(\Delta V)}. \quad (11)$$

Substituting equation 9 into equation 11 results in the Kelvin equation in a more general form than usually seen:

$$RT \ln(p/p_\infty) = V_m \sum_i \sigma_i \frac{\delta(\Delta A_i)}{\delta(\Delta V)}. \quad (12)$$

The Kelvin equation states that if the embryo-vapor system is to be in equilibrium, the chemical potential of the substance in the vapor must be larger than its chemical potential when in equilibrium with a large enough quantity of the condensed phase so that surface effects are negligible. The difference is due to the surface free energy and the curvature of the surface of the embryo.

The free energy change of the system for the formation of an embryo becomes

$$\Delta G = -RT \ln(p/p_\infty) \frac{\Delta V}{V_m} + \sum_i \sigma_i \Delta A_i \quad (13)$$

When the ratio p/p_∞ is greater than unity, the interaction of the right-hand terms of equation 13 leads to a maximum value of $\underline{\Delta G}$ at some volume change, the critical change in volume, $\underline{\Delta V^*}$. Differentiating equation 13 with respect to $\underline{\Delta V}$ and setting the differential to zero, evaluation at the critical volume change yields

$$\sum_i \sigma_i \left(\frac{\partial \Delta A_i}{\partial \Delta V} \right)_{\Delta V^*} = \frac{RT \ln(p/p_\infty)}{V_m} \quad (14)$$

That a maximum in $\underline{\Delta G}$ exists is significant. Once formed, an embryo must increase in volume to grow. If the volume of the embryo after it is formed, is less than the critical volume, growth would be accompanied by a positive change in the free energy of the system. However, a process for which the free energy of the system increases is not thermodynamically feasible in a statistical sense. But, if the volume of the embryo after it is formed is equal to or greater than the critical volume, growth would lead to a reduction in the free energy of the system. The critical volume is the lower size limit for embryos which may spontaneously grow into larger drops. The critical free energy is the energy barrier which must be overcome to form embryos of this size.

Throughout the derivation of equations 13 and 14 no reference is made to homogeneous or heterogeneous nucleation. These equations are completely general since no assumptions are made about the nature of the process or geometry of the embryo

other than that the embryo is an aggregation of molecules. Assumptions have been made on the nature of the thermodynamic properties of the embryo such that these properties were taken to be the same as for the condensed phase. Two of the more common applications of equations 13 and 14 are presented below. These are by no means the only nucleation processes to which these equations can be applied. Nucleation at lattice step sites, on curved surfaces, nucleation of the solid phase, both homogeneous and heterogeneous, are some of the nucleation processes that are governed by these equations. Applying these equations to physical systems is possible only if information on the surface free energies is available.

Homogeneous Nucleation

The formation of an embryo in a system containing only one chemical species and, initially, only one phase is called homogeneous nucleation. In this case equation 13 becomes

$$\Delta G = -RT \ln(p/p_{\infty}) \frac{\Delta V}{V_m} + \sigma_{L, V} \Delta A_{L, V} \quad (15)$$

where the subscripts $\underline{L, V}$ denote the nature of the interface, i. e., for the condensation of a vapor to the liquid, the liquid-vapor interface. The surface free energy of a liquid-vapor interface is identical to the surface tension. Only one surface area and surface free energy is involved in homogeneous nucleation. Equation 14 becomes

$$\left(\frac{\partial \Delta A}{\partial \Delta V} \right)_{\Delta V^*} = \frac{RT \ln(p/p_{\infty})}{\sigma_{L, V} V_m} \quad (16)$$

Heterogeneous Nucleation

If in the initial state of the system more than one phase is present, i. e. , the pure vapor and a solid phase, the formation of an embryo on this solid is called heterogeneous nucleation. By assuming the solid has the form of a plane substrate, three surface areas and surface free energies are involved such that equation 13 becomes

$$\Delta G = -RT \ln(p/p_{\infty}) \frac{\Delta V}{V_m} + \sigma_{L, V} \Delta A_{L, V} + \sigma_{S, L} \Delta A_{S, L} + \sigma_{S, V} \Delta A_{S, V} \quad (17)$$

where the subscripts, as above, refer to the nature of the interface. The surface areas involving the solid substrate are related such that

$$\Delta A_{S, V} = - \Delta A_{S, L} .$$

Substituting this relation into equation 17 yields

$$\Delta G = -RT \ln(p/p_{\infty}) \frac{\Delta V}{V_m} + \sigma_{L, V} \Delta A_{L, V} + (\sigma_{S, L} - \sigma_{S, V}) \Delta A_{S, L} \quad (18)$$

The Young-Dupré equation gives the relation between the surface free energies used in equation 18 and the contact angle θ of the bulk liquid on the solid substrate as

$$\frac{\sigma_{S, V} - \sigma_{S, L}}{\sigma_{L, V}} = \cos \theta$$

Using this concept of contact angle, equation 18 becomes

$$\Delta G = -RT \ln(p/p_\infty) \frac{\Delta V}{V_m} + \sigma_{L,V} (\Delta A_{L,V} - \cos \theta \Delta A_{S,L}) \quad (19)$$

which is the free energy change for the formation of an embryo by heterogeneous nucleation on a plane substrate as given by Volmer (1939, and cited by Fletcher (1962)).

Proceeding in a similar fashion, equation 14 for heterogeneous nucleation becomes

$$\left(\frac{\partial (\Delta A_{L,V} - \cos \theta \Delta A_{S,L})}{\partial \Delta V} \right)_{\Delta V^*} = \frac{RT \ln(p/p_\infty)}{\sigma_{L,V} V_m} \quad (20)$$

if the contact angle is independent of the volume of the embryo.

SPHERICAL APPROXIMATION OF THE EMBRYO SHAPE

A natural choice for a first approximation to the shape of an embryo is a sphere. For homogeneous nucleation the embryo is assumed to be a sphere, while for heterogeneous nucleation the embryo is taken to be a segment of a sphere.

Homogeneous Nucleation

The spherical embryo in the homogeneous case is assumed to have a radius r . Substituting the volume and surface area of a sphere into equation 15 gives

$$\Delta G = -RT \ln(p/p_{\infty}) \frac{4\pi r^3}{3V_m} + \sigma_{L,V} 4\pi r^2 \quad (21)$$

and equation 16 becomes

$$\left(\frac{\partial \Delta A_{L,V}}{\partial \Delta V} \right)_{\Delta V^*} = \frac{2}{r^*} = \frac{RT \ln(p/p_{\infty})}{\sigma_{L,V} V_m}$$

or

$$r^* = \frac{2\sigma_{L,V} V_m}{RT \ln(p/p_{\infty})} \quad (22)$$

where r^* is the critical radius. These equations are given by Gibbs (1906), Frenkel (1946), Volmer and Weber (1926) and cited by Fletcher (1962) and are most often derived in a less general manner by introducing the spherical shape into equation 4.

Heterogeneous Nucleation

The embryo in heterogeneous nucleation is taken to be a spherical cap resting on a solid, plane, insoluble substrate as shown in figure 1. Adamson and Ling (1964) point out that the surface of the substrate must be homogeneous if the embryo is to be a volume of revolution. The contact angle plays an important role in determining the volume and surface areas of an embryo of given radius of curvature. The volume and surface areas are found to be

$$\Delta A_{L, V} = 2\pi r^2 (1 - \cos \theta) \quad (23a)$$

$$\Delta A_{S, L} = \pi r^2 (1 - \cos^2 \theta) \quad (23b)$$

$$\Delta V = \frac{\pi r^3}{3} (2 + \cos \theta) (1 - \cos \theta)^2 \quad (23c)$$

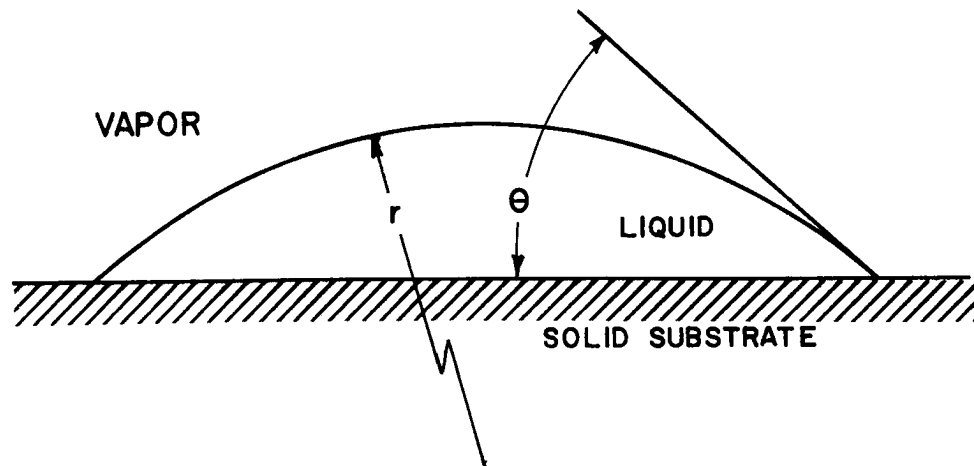


Figure 1. The spherical cap heterogeneous nucleation embryo

Substituting equations 23 into equation 19 gives

$$\Delta G = \left(-RT \ln(p/p_{\infty}) \frac{4\pi r^3}{3} + \sigma_{L, V} 4\pi r^2 \right) f(\theta) \quad (24)$$

where $f(\theta) = (2 + \cos \theta)(1 - \cos \theta)^2/4$. Notice that the free energy change for heterogeneous nucleation on a plane substrate differs from that for homogeneous nucleation only by the factor $f(\theta)$ which is dependent on the contact angle alone. Using the spherical cap approximations equation 20 reduces to the same expression as given by homogeneous nucleation,

$$r^* = \frac{2\sigma_{L, V} V_m}{RT \ln(p/p_{\infty})} \quad (25)$$

Volmer (1939, and cited by Fletcher (1962)) also arrives at equations 24 and 25 and concludes that the influence of an inert, plane substrate on nucleation is to reduce the free energy barrier to the formation of the critical embryo but not to change the critical radius of the embryo.

Nonspherical Shapes

Examination of equation 16 gives some insight on the effect of a nonspherical shape of the embryo on the results obtained by the spherical approximation for homogeneous nucleation. It is well known that the differential $(\partial A/\partial V)$ is a minimum for a sphere and that all other shapes give rise to values of $(\partial A/\partial V)$ larger than

that for the sphere. Therefore, to obtain the same critical volume at the same temperature the ratio p/p_∞ must be larger for non-spherical embryo shapes.

Such an easy analysis for the heterogeneous case is not possible since more information on the surface area-volume relations is needed. The next section will investigate a more realistic shape for the embryo in the process of heterogeneous nucleation on a plane substrate. By comparing the free energy change expressions for the nonspherical embryo to that for the spherical cap as shown in equation 24, the accuracy of the spherical cap approximation can be determined.

THE SESSILE DROP

To investigate the influence of a nonspherical drop shape on nucleation consider a sessile drop resting on top of a plane, horizontal, insoluble homogeneous substrate under the action of gravity and in equilibrium with its vapor. Bashforth and Adams (1883) point out that the differential equation describing the shape of the sessile drop as a function of the size and surface tension of the drop has been derived by Laplace, Gauss, and Young by very different approaches, each resulting in the same set of equations. A straightforward derivation on the basis of mechanical statics alone with no inference as to the origin of the surface tension of the liquid-vapor interface follows.

By symmetry the drop surface will be a surface of revolution about a vertical axis, parallel to the action of gravity. A vertical section through the axis of revolution is presented in figure 2 with the contact angle exaggerated. The principal radii of curvature are given by ρ in the plane of the paper and by $x/\sin\phi$ normal to the plane of the paper. The angle ϕ varies from zero at the vertex to θ , the contact angle of the liquid on the substrate.

By the Young-Laplace equation the difference in pressure across a curved fluid surface is

$$\Delta p = \sigma_{L, V} \left(\frac{1}{R_1} + \frac{1}{R_2} \right) \quad (26)$$

where \underline{R}_1 and \underline{R}_2 are the principal radii of curvature. Because of the action of gravity a hydrostatic pressure within the drop contributes to the pressure difference such that

$$\Delta p = \underline{d}gz + C \quad (27)$$

where \underline{d} is the density, \underline{g} the acceleration of gravity and \underline{C} an arbitrary constant. Equating equations 26 and 27 and substituting for the principal radii yields

$$\underline{d}gz + C = \sigma_{L, V} \left(\frac{1}{\rho} + \frac{\sin \phi}{x} \right) . \quad (28)$$

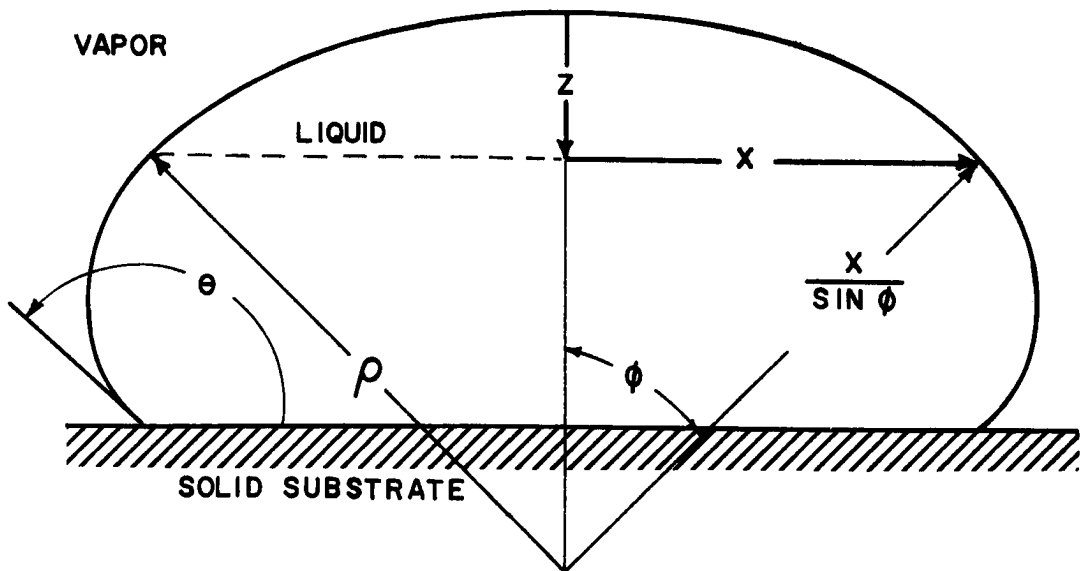


Figure 2. The sessile drop

At the origin the two radii of curvature are equal to the radius of curvature at the vertex, \underline{b} , i. e. ,

$$\lim_{z \rightarrow 0} \rho = \lim_{z \rightarrow 0} \frac{x}{\sin \phi} = b .$$

This fixes the value of \underline{C} such that

$$gdz + \frac{2}{b} = \sigma_{L, V} \left(\frac{1}{\rho} + \frac{\sin \phi}{x} \right) . \quad (29)$$

By dividing the variables \underline{x} , \underline{z} , and $\underline{\rho}$ by the parameter \underline{b} , equation 29 is nondimensionalized to

$$\frac{1}{\rho} + \frac{\sin \phi}{x} = 2 + \beta z \quad (30)$$

where

$$\beta = \frac{gdb^2}{\sigma_{L, V}} .$$

Equation 30 gives the shape of the sessile drop in terms of three nondimensional coordinates \underline{x} , \underline{z} , and $\underline{\rho}$ and the shape parameter $\underline{\beta}$.

A differential equation involving only \underline{x} and \underline{z} can be obtained by substituting the differential forms for $\underline{\rho}$ and $\underline{\sin \phi}$

$$\rho = \left(1 + \left(\frac{dz}{dx} \right)^2 \right)^{3/2} / \frac{d^2 z}{dx^2}$$

$$\sin \phi = \frac{dz}{dx} / \left(1 + \left(\frac{dz}{dx} \right)^2 \right)^{1/2}$$

to yield

$$\frac{d^2 z}{dx^2} + \left(1 + \left(\frac{dz}{dx} \right)^2 \right) \frac{1}{x} \frac{dz}{dx} = (2 + \beta z) \left(1 + \left(\frac{dz}{dx} \right)^2 \right)^{3/2}. \quad (31)$$

Equation 31 is a non-linear, second degree and order two differential equation; a closed form solution is impossible. This differential equation along with the equations

$$dx = \rho \cos \phi \, d\phi$$

$$dz = \rho \sin \phi \, d\phi$$

form a set of differential equations describing the sessile drop which can be solved by series techniques.

Bashforth and Adams (1883) obtained solutions for the variables \underline{x} , \underline{z} , $\underline{\rho}$, and $\underline{1/\rho}$ as power series of the variables $\underline{\phi}$ and $\underline{\beta}$. These solutions are given in Appendix I. From these solutions, which are exact provided that $\underline{\phi}$ and $\underline{\beta}$ are small so that the series converge rapidly, the surface areas and volume needed in equation 19 can be derived.

The area of the interface between the substrate and embryo is found to be

$$\begin{aligned} \Delta A_{S,L} = \pi x^2 = \pi b^2 & \left[\theta^2 - \left(\frac{1}{3} + \frac{1}{4}\beta \right) \theta^4 + \left(\frac{2}{45} + \frac{1}{8}\beta + \frac{19}{192}\beta^2 \right) \theta^6 \right. \\ & - \left(\frac{1}{315} + \frac{13}{960}\beta + \frac{35}{576}\beta^2 + \frac{217}{4608}\beta^3 \right) \theta^8 + \left(\frac{2}{14175} + \frac{311}{120960}\beta + \frac{2029}{138240}\beta^2 \right. \\ & + \left. \frac{4597}{138240}\beta^3 + \frac{3043}{122880}\beta^4 \right) \theta^{10} - \left(\frac{2}{467775} + \frac{437}{2419200}\beta + \frac{1997}{967680}\beta^2 \right. \\ & \left. + \frac{15841}{1658880}\beta^3 + \frac{35927}{184320}\beta^4 + \frac{306703}{22118400}\beta^5 \right) \theta^{12} + \dots \right]. \quad (32) \end{aligned}$$

The area of the liquid-vapor interface is given by the integral

$$\Delta A_{L, V} = \int_0^\theta 2\pi x \rho d\phi$$

which leads to

$$\begin{aligned} \Delta A_{L, V} = & \pi b^2 \left[\theta^2 - \left(\frac{1}{12} + \frac{1}{4}\beta \right) \theta^4 + \left(\frac{1}{360} + \frac{1}{24}\beta + \frac{19}{192}\beta^2 \right) \theta^6 \right. \\ & - \left(\frac{1}{20160} + \frac{1}{320}\beta + \frac{109}{4608}\beta^2 + \frac{217}{4608}\beta^3 \right) \theta^8 + \left(\frac{1}{181440} + \frac{17}{120960}\beta \right. \\ & + \frac{379}{138240}\beta^2 + \frac{1993}{138240}\beta^3 + \frac{3043}{122880}\beta^4 \left. \right) \theta^{10} - \left(\frac{1}{239500800} + \frac{31}{7257600}\beta \right. \\ & \left. + \frac{757}{3870720}\beta^2 + \frac{1853}{829440}\beta^3 + \frac{67633}{7372800}\beta^4 + \frac{306703}{22118400}\beta^5 \right) \theta^{12} + \dots \left. \right] . \end{aligned} \quad (33)$$

The volume of the sessile drop can be found by differentiating equation 30 to give

$$\beta dz = \frac{d\rho}{\rho} + \frac{\cos\phi}{x} d\phi - \frac{\sin\phi}{x^2} dx .$$

For a volume of revolution, a volume element can be represented as

$$dV = \pi x^2 dz$$

thus

$$dV = \frac{\pi}{\beta} - \frac{x^2}{\rho} d\rho + x \cos\phi d\phi - \sin\phi dx . \quad (34)$$

Integrating by parts and using the differential relation

$$dx = \rho \cos\phi d\phi$$

the volume is found to be

$$V = \frac{\pi}{\beta} \left(\frac{x^2}{\rho} - x \sin \phi \right). \quad (35)$$

Algebraically combining the series forms of the terms in equation 35,

the volume of the sessile drop becomes

$$\begin{aligned} V = \pi b^3 & \left[\frac{1}{4} \theta^4 - \left(\frac{1}{12} + \frac{5}{48} \beta \right) \theta^6 + \left(\frac{13}{960} + \frac{3}{64} \beta + \frac{77}{1536} \beta^2 \right) \theta^8 \right. \\ & - \left(\frac{41}{30240} + \frac{23}{2304} \beta + \frac{157}{5760} \beta^2 + \frac{271}{10240} \beta^3 \right) \theta^{10} + \left(\frac{671}{7257600} + \frac{479}{362880} \beta \right. \\ & \left. \left. + \frac{7771}{1105920} \beta^2 + \frac{9157}{552960} \beta^3 + \frac{131329}{8847360} \beta^4 \right) \theta^{12} - \dots \right]. \quad (36) \end{aligned}$$

As they now stand, equations 32, 33, and 36 do not give any insight into the departure from sphericity of the surface areas and volume of the sessile drop without a more detailed examination of the spherical cap. However, by expanding equations 23 as power series in θ , the surface area and volume of the spherical cap become

$$\begin{aligned} (\Delta A_{S, L})_S &= \pi r^2 \left[\theta^2 - \frac{1}{3} \theta^4 + \frac{2}{45} \theta^6 - \frac{1}{315} \theta^8 + \frac{2}{14175} \theta^{10} \right. \\ & \left. - \frac{2}{467775} \theta^{12} + \dots \right] \quad (37) \end{aligned}$$

$$\begin{aligned} (\Delta A_{L, V})_S &= \pi r^2 \left[\theta^2 - \frac{1}{12} \theta^4 + \frac{1}{360} \theta^6 - \frac{1}{20160} \theta^8 + \frac{1}{181440} \theta^{10} \right. \\ & \left. - \frac{1}{239500800} \theta^{12} + \dots \right] \quad (38) \end{aligned}$$

$$\begin{aligned} (\Delta V)_S &= \pi r^3 \left[\frac{1}{4} \theta^4 - \frac{1}{12} \theta^6 + \frac{13}{960} \theta^8 - \frac{41}{30240} \theta^{10} + \frac{671}{7257600} \theta^{12} - \dots \right] \quad (39) \end{aligned}$$

where the subscript \underline{s} refers to the spherical cap. Comparing equations 32 and 37, 33 and 38, and 36 and 39 it is apparent that the sessile drop shape can be represented as a spherical cap plus correction terms to account for the departure from a spherical shape. When the parameter $\underline{\beta}$ or the contact angle becomes small the sessile drop reduces to a spherical cap. $\underline{\beta}$ becomes small for small drops or in the absence of gravity since $\underline{\beta}$ is really a measure of the hydrostatic pressure within the drop that causes the departure from sphericity.

THE SESSILE DROP AS AN EMBRYO

The series forms for the surface areas and volume of the sessile drop are substituted into equation 19 to give the free energy change of the system for the formation of an embryo shaped as a sessile drop. By writing the volume and surface areas as a sum of the corresponding spherical cap term and series correction terms the free energy change becomes

$$\begin{aligned}
\Delta G_{\text{sessile drop}} = & \frac{-RT \ln(p/p_{\infty})}{V_m} \left\{ \left(\Delta V \right)_s - \beta b^3 \theta^6 \left[\frac{5}{48} - \left(\frac{3}{64} + \frac{77}{1536} \beta \right) \theta^2 \right. \right. \\
& + \left. \left(\frac{23}{2304} + \frac{157}{5760} \beta + \frac{271}{10240} \beta^2 \right) \theta^4 - \left(\frac{479}{362880} + \frac{7771}{1105920} \beta + \frac{9157}{552960} \beta^2 \right. \right. \\
& + \left. \left. \frac{131329}{8847360} \beta^3 \right) \theta^6 + \dots \right\} + \sigma_{L, V} \left\{ \left(\Delta A_{L, V} \right)_s - \beta b^2 \theta^4 \left[\frac{1}{4} - \left(\frac{1}{24} \right. \right. \right. \\
& + \left. \left. \frac{19}{192} \beta \right) \theta^2 + \left(\frac{1}{320} + \frac{109}{4608} \beta + \frac{217}{4608} \beta^2 \right) \theta^4 - \left(\frac{17}{120960} + \frac{379}{138240} \beta \right. \right. \\
& + \left. \left. \frac{1993}{138240} \beta^2 + \frac{3043}{122880} \beta^3 \right) \theta^6 + \left(\frac{31}{7257600} + \frac{757}{3870720} \beta + \frac{1853}{829440} \beta^2 \right. \right. \\
& + \left. \left. \frac{67633}{7372800} \beta^3 + \frac{306703}{22118400} \beta^4 \right) \theta^8 - \dots \right\} - \sigma_{L, V} \cos \theta \left\{ \left(\Delta A_{S, L} \right)_s \right. \\
& - \beta b^2 \theta^4 \left[\frac{1}{4} - \left(\frac{1}{8} + \frac{19}{192} \beta \right) \theta^2 + \left(\frac{13}{960} + \frac{35}{576} \beta + \frac{217}{4608} \beta^2 \right) \theta^4 - \left(\frac{311}{120960} \right. \right. \\
& + \left. \left. \frac{2029}{138240} \beta + \frac{4597}{138240} \beta^2 + \frac{3043}{122880} \beta^3 \right) \theta^6 + \left(\frac{437}{2419200} + \frac{1997}{967680} \beta \right. \right. \\
& + \left. \left. \frac{15841}{1658880} \beta^2 + \frac{35927}{184320} \beta^3 + \frac{306703}{22118400} \beta^4 \right) \theta^8 - \dots \right\} . \quad (40)
\end{aligned}$$

The spherical cap terms may be combined as in equation 24 and the series terms for the surface area corrections may be combined to give

$$\Delta G_{\text{sessile drop}} = \Delta G_{\text{spherical cap}} - \Delta \quad (41)$$

In assuming the free energy change for the spherical cap is that for the sessile drop, the error is

$$\Delta = \pi g d \theta^6 r^*{}^4 x^4 (-xV_c + A_c) \quad (42)$$

where

$$x = \frac{b}{r^*}$$

$$r^* = \frac{2\sigma_{L,V} V_m}{RT \ln(p/p_\infty)}$$

$$\begin{aligned} V_c = & \frac{5}{24} - \left(\frac{3}{32} + \frac{154}{1536} \beta \right) \theta^2 + \left(\frac{23}{1152} + \frac{157}{2880} \beta + \frac{271}{5120} \beta^2 \right) \theta^4 \\ & - \left(\frac{479}{181440} + \frac{7771}{552960} \beta + \frac{9157}{276480} \beta^2 + \frac{131329}{4423680} \beta^3 \right) \theta^6 + \dots \end{aligned} \quad (43)$$

and

$$\begin{aligned} A_c = & \frac{5}{24} - \left(\frac{3}{32} + \frac{133}{1536} \beta \right) \theta^2 + \left(\frac{23}{1152} + \frac{107}{2304} \beta + \frac{217}{5120} \beta^2 \right) \theta^4 \\ & - \left(\frac{479}{181440} + \frac{2189}{18432} \beta + \frac{3581}{138240} \beta^2 + \frac{33473}{1474560} \beta^3 \right) \theta^6 + \dots \end{aligned} \quad (44)$$

The term containing $\underline{V_c}$ gives that portion of $\underline{\Delta}$ which is due to the difference in volume between the spherical cap and the sessile drop while the term containing $\underline{A_c}$ gives that portion of $\underline{\Delta}$ due to the surface area differences.

Equation 42 may be further simplified by noting that

\underline{V}_c is always larger than \underline{A}_c , thus

$$\Delta = \pi g d \theta^6 r^*{}^4 x^4 \left[(1-x) \underline{A}_c + x \beta \theta^2 (\underline{A}_c - \underline{V}_c) \right] \quad (45)$$

where

$$\begin{aligned} (\underline{A}_c - \underline{V}_c) = & \frac{7}{512} - \left(\frac{31}{3840} + \frac{27}{2560} \beta \right) \theta^2 + \left(\frac{301}{13824} + \frac{133}{18432} \beta \right. \\ & \left. + \frac{3091}{442368} \beta^2 \right) \theta^4 - \dots \quad (46) \end{aligned}$$

The term $(1-x)\underline{A}_c$ represents the interaction of the volume and surface area differences between the spherical cap and sessile drop. Physical interpretation of this term for $\underline{x} < 1$ is that the difference in surface area between the sessile drop and spherical cap plays the major role in the error while for values of $\underline{x} > 1$ the difference in volume plays the greatest role. The remaining term, $\underline{x} \beta \theta^2 (\underline{A}_c - \underline{V}_c)$, indicates that the volume difference always plays a role in $\underline{\Delta}$ and is the residual error when $\underline{x} = 1$.

By writing the free energy change for the spherical cap, equation 24, as

$$\Delta G_{\text{spherical cap}} = \pi \sigma_{L,V} \left(1 - \frac{2}{3}x\right) x^2 r^*{}^2 f(\theta) \quad (47)$$

the relative error in assuming the free energy change for the sessile drop to be given by that for the spherical cap is

$$\delta = \frac{\Delta}{\Delta G_{\text{spherical cap}}}$$

$$\delta = \frac{gd\theta^6 r^{*2}}{\sigma_{L, V} f(\theta)} \frac{x^2}{(1 - \frac{2}{3}x)} \left[(1 - x)A_c + K(A_c - V_c)x^3 \right] \quad (48)$$

where

$$K = \frac{gd\theta^2 r^{*2}}{\sigma_{L, V}} = \frac{4gd\sigma_{L, V}\theta^2 V_m^2}{[RT \ln(p/p_\infty)]^2}$$

Use of equation 48 is limited to values of $\underline{x} < 3/2$ since at this value $\underline{\delta}$ becomes infinite.

Examination of the equations for $\underline{\Delta}$ and $\underline{\delta}$ indicates that a maximum for each should occur at some value of \underline{x} . These maxima are found by differentiating equations 45 and 48 with respect to \underline{x} , setting the differentials to zero and solving for \underline{x} . By assuming $\underline{\beta}$ to be small the terms \underline{V}_c and \underline{A}_c can be considered independent of \underline{x} . The value of \underline{x} for a maximum in $\underline{\Delta}$ is given by

$$4 - 5x + 7K \frac{(A_c - V_c)}{A_c} x^3 = 0 \quad (49)$$

while that for a maximum in $\underline{\delta}$ is given by

$$6 - 11x + 4x^2 + K \frac{(A_c - V_c)}{A_c} (15x^3 - 8x^4) = 0 \quad (50)$$

For most real systems the value of \underline{K} is much less than unity so that equations 49 and 50 can be written as

$$4 - 5x = 0$$

for $\underline{\Delta}_{\max}$ and

$$6 - 11x + 4x^2 = 0$$

for $\underline{\delta}_{\max}$ or

$$x_{\Delta_{\max}} = .8$$

$$x_{\delta_{\max}} = .75 .$$

Because the term $(1 - x)A_c$ changes sign as \underline{x} increases beyond unity both $\underline{\Delta}$ and $\underline{\delta}$ must have zeros at some value of \underline{x} .

Setting the bracketed factor in equation 48 to zero gives

$$1 - K \frac{(A_c - V_c)}{A_c} x^3 = x \quad (51)$$

and for $\underline{K} < 1$ as discussed above the zero must be very near to but just slightly greater than $\underline{x} = 1$. Thus $\underline{\Delta G}_{\text{spherical cap}}$ is an over-estimation of $\underline{\Delta G}_{\text{sessile drop}}$ for values of $\underline{x} < 1$ and an underestimation for $\underline{x} > 1$.

The dependence of $\underline{\Delta}$ and $\underline{\delta}$ on the physical parameters temperature, supersaturation, contact angle, density, and surface tension can be seen by examining the coefficients of the terms in \underline{x} of equations 45 and 48

$$\Delta = \pi g \bar{u} r^* \theta^6 g(x, \theta, \beta)$$

$$\delta = \frac{g \bar{d} r^* \theta^6}{\sigma_{L, V} f(\theta)} h(x, \theta, \beta)$$

where $\underline{g(x, \theta, \beta)}$ and $\underline{h(x, \theta, \beta)}$ are given in equations 45 and 48.

Substituting for $\underline{r^*}$ these equations become

$$\Delta = \frac{16\pi gM^4 \sigma_{L, V}^4 \theta^6}{d^3 RT \ln(p/p_\infty)^4} g(x, \theta, \beta) \quad (52)$$

$$\delta = \frac{4gM^2 \sigma_{L, V} \theta^6}{[RT \ln(p/p_\infty)]^2 df(\theta)} h(x, \theta, \beta) \quad (53)$$

where M is the gram-molar weight and clearly shows how $\underline{\Delta}$ and $\underline{\delta}$ depend on the physical parameters. Since $\underline{\beta}$ is defined as

$$\beta = \frac{gdb^2}{\sigma_{L, V}}$$

then

$$\beta^* = \frac{gdr^{*2}}{\sigma_{L, V}} x^2 .$$

Both $\underline{\Delta}$ and $\underline{\delta}$ approach zero as $\underline{\beta^*}$, $\underline{\theta}$, or \underline{g} become small. This result agrees with the behavior of the volume and surface areas of the sessile drop at small values of $\underline{\beta}$, $\underline{\theta}$, and \underline{g} ; they reduce to the spherical cap values and so does the free energy change for the formation of an embryo.

NUMERICAL COMPUTATIONS

Using the computer program presented in Appendix II numerical values of the error in assuming the free energy change of the system for the formation of a sessile drop embryo is given by the free energy change for a spherical cap were computed for two contrasting systems: water and mercury. Since surface tension data is readily available for water the errors were computed at two temperatures. However, only one value of the surface tension of mercury was found in the literature. Errors were computed for supersaturations ranging from 0.1 to 1000 percent, for contact angles from 11.5 to 57.3 degrees, and for values of \underline{x} from 0.05 to 1.5.

Figure 3 illustrates the variation of $\underline{\Delta}$ with \underline{x} and clearly shows the maximum occurring at $\underline{x} = 0.8$. As equation 52 indicates, a higher temperature gives smaller errors. This trend is seen throughout the remaining graphs. At a given supersaturation, contact angle, and \underline{x} , say at the maximum, equation 52 can be modified to give the relationship between the $\underline{\Delta}$'s at two different temperatures as

$$\frac{\Delta_1}{\Delta_2} = \left(\frac{\sigma_{L, V_1} T_2}{\sigma_{L, V_2} T_1} \right)^4 \left(\frac{d_2}{d_1} \right)^3 . \quad (54)$$

For water the constants are

$$T_1 = 25^\circ\text{C}, \quad \sigma_{L, V_1} = 71.97 \text{ erg/cm}^2, \quad d_1 = 0.99987 \text{ gm/cm}^3$$

$$T_2 = 0^\circ\text{C}, \quad \sigma_{L, V_2} = 74.92 \text{ erg/cm}^2, \quad d_2 = 0.9970 \text{ gm/cm}^3$$

and the ratio $\underline{\Delta_1/\Delta_2} = 0.605$, which is equal to that using the computed data.

The variation of the relative error with size is shown in figure 4 for 0.1 percent supersaturation and a contact angle of 34.4 degrees. As with $\underline{\Delta}$, $\underline{\delta}$ has a maximum at the predicted value, $\underline{x} = 0.75$. Higher temperatures reduce the relative error. Using equation 53 in a modified form the relationship between $\underline{\delta}$'s at different temperatures for a given supersaturation, contact angle, and \underline{x} , again taken for the maximum $\underline{\delta}$, is

$$\frac{\delta_1}{\delta_2} = \left(\frac{d_2 \sigma_{L, V_1}}{d_1 \sigma_{L, V_2}} \right) \left(\frac{T_2}{T_1} \right)^2. \quad (55)$$

Using the values given above for water the ratio $\underline{\delta_1/\delta_2} = 0.809$ which is the same as that given by the computed data. The ratios $\underline{\Delta_1/\Delta_2}$ and $\underline{\delta_1/\delta_2}$ are valid only when $\underline{g(x, \theta, \beta)}$ and $\underline{h(x, \theta, \beta)}$ are not nearly zero, i. e., $\underline{x} \ll 1$ or $\underline{x} \gg 1$ but not $\underline{x} \approx 1$.

Since the relative error is perhaps the more useful measure of the error made by using the free energy change for the spherical cap as that for the sessile drop figures 5, 6, 7, and 8

show how $\underline{\delta}$ varies with supersaturation and contact angle at the maximum and at the critical radius. The small circle and triangle at the vertex of the 0°C and 25°C curves in figure 4 are placed at the corresponding points on the other curves. Figure 5 clearly shows how small the maximum relative error is and that $\underline{\delta}$ decreases rapidly with increasing supersaturation. The relative error at the critical radius is shown in figure 6 and is several orders of magnitude smaller than the maximum relative error. Curves at other contact angles are parallel to the curves in figures 5 and 6. Figure 7 shows that the maximum relative error vanishes for small contact angles and that in the range of contact angles for which this study is valid the maximum relative error is negligibly small. At the critical radius the relative error as a function of contact angle is shown in figure 8. Curves for other supersaturations are parallel to the curves of the relative error in figures 7 and 8.

In order to find a substance which would serve as a comparison to water equations 52 and 53 were manipulated to give the ratios of $\underline{\Delta}$ and $\underline{\delta}$ for different substances at the same temperature, supersaturation, contact angle, and size as

$$\frac{\Delta_1}{\Delta_2} = \left(\frac{d_2}{d_1} \right)^3 \left(\frac{\sigma_{L, V_1} M_1}{\sigma_{L, V_2} M_2} \right)^4 \quad (56)$$

and

$$\frac{\delta_1}{\delta_2} = \left(\frac{d_2 \sigma_{L, V_1}}{d_1 \sigma_{L, V_2}} \right) \left(\frac{M_1}{M_2} \right)^2 \quad (57)$$

Comparing substances of known surface tension to water, mercury was found to give the largest ratios. The data for mercury that were used in the computations are for a temperature of 25° C:

$$M_{\text{Hg}} = 200.61 \text{ gm/mole}, \quad \sigma_{L, V_{\text{Hg}}} = 484.0 \text{ erg/cm}^2,$$

$$d_{\text{Hg}} = 13.534 \text{ gm/cm}^3.$$

Using these values the ratio $\frac{\Delta_{\text{Hg}}}{\Delta_{\text{H}_2\text{O}}} = 1.27 \times 10^4$ and

$$\frac{\delta_{\text{Hg}}}{\delta_{\text{H}_2\text{O}}} = 61.6.$$

A graph comparing $\underline{\Delta}$ for water and mercury is found to be impractical because of the very large difference in magnitude of the errors. However, a graphical comparison of $\underline{\delta}$ is feasible and is shown in figure 9. Using the computed data the ratios $\frac{\Delta_{\text{Hg}}}{\Delta_{\text{H}_2\text{O}}}$ and $\frac{\delta_{\text{Hg}}}{\delta_{\text{H}_2\text{O}}}$ agree very closely with the values presented above. By virtue of the logarithmic presentation a comparison of the maximum relative error for water and for mercury is much more descriptive of the great difference in error as shown in figure 10 as a function of the supersaturation. This figure again points out the very negligible error even for the worst system investigated. Figure 11 compares the contact angle dependence of $\underline{\delta}$ for mercury and water and again emphasizes the great difference between the two systems. The small circle and triangle at the

maximum of each curve in figure 9 are located at corresponding points in figures 10 and 11.

The computer generated data used for drawing these graphs is presented in tabular form in Appendix III.

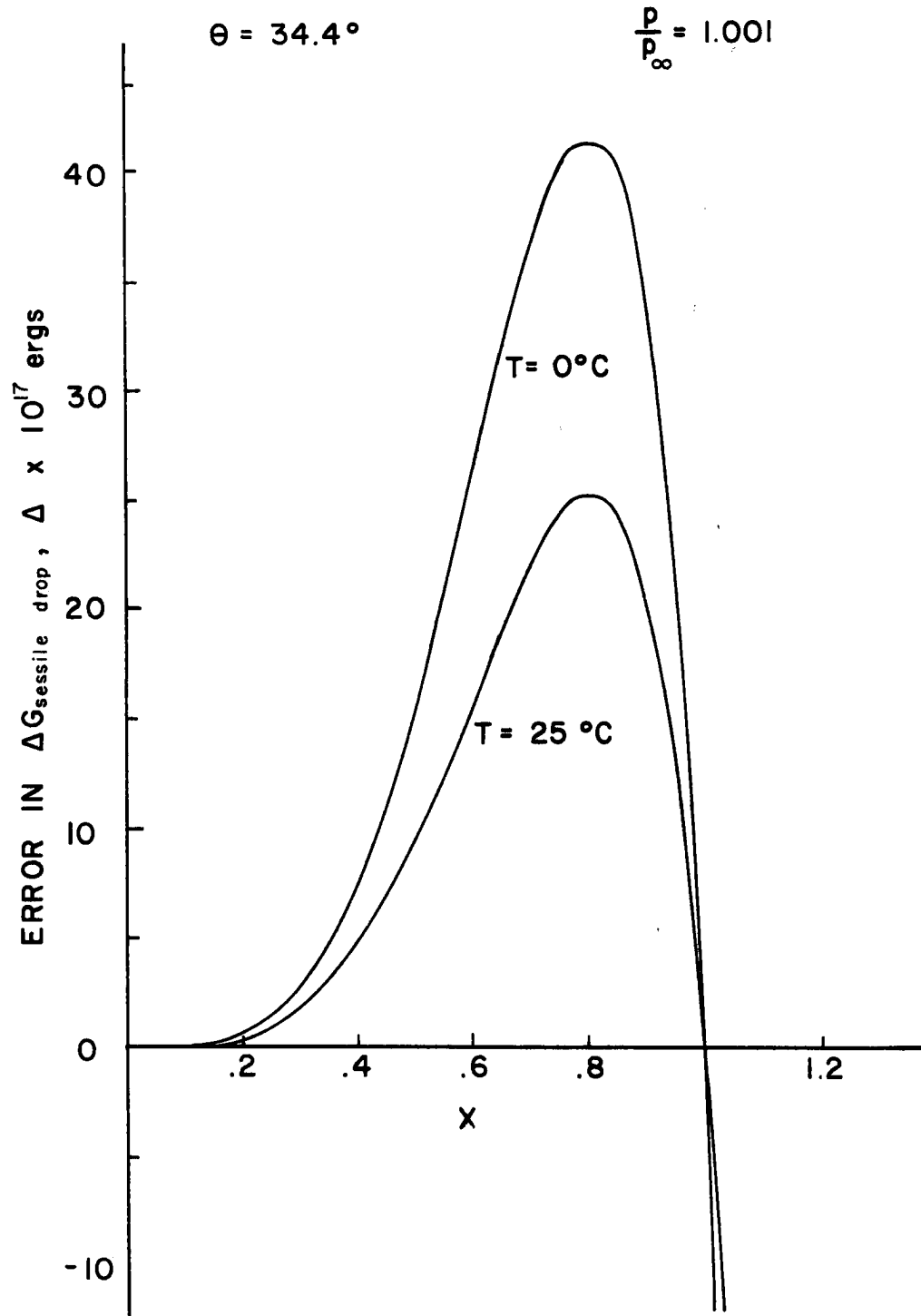


Figure 3. The error in assuming $\Delta G_{\text{sessile drop}}$ is given by $\Delta G_{\text{spherical cap}}$ for 0.1 percent supersaturation and a contact angle of 34.4 degrees as a function of \underline{X}

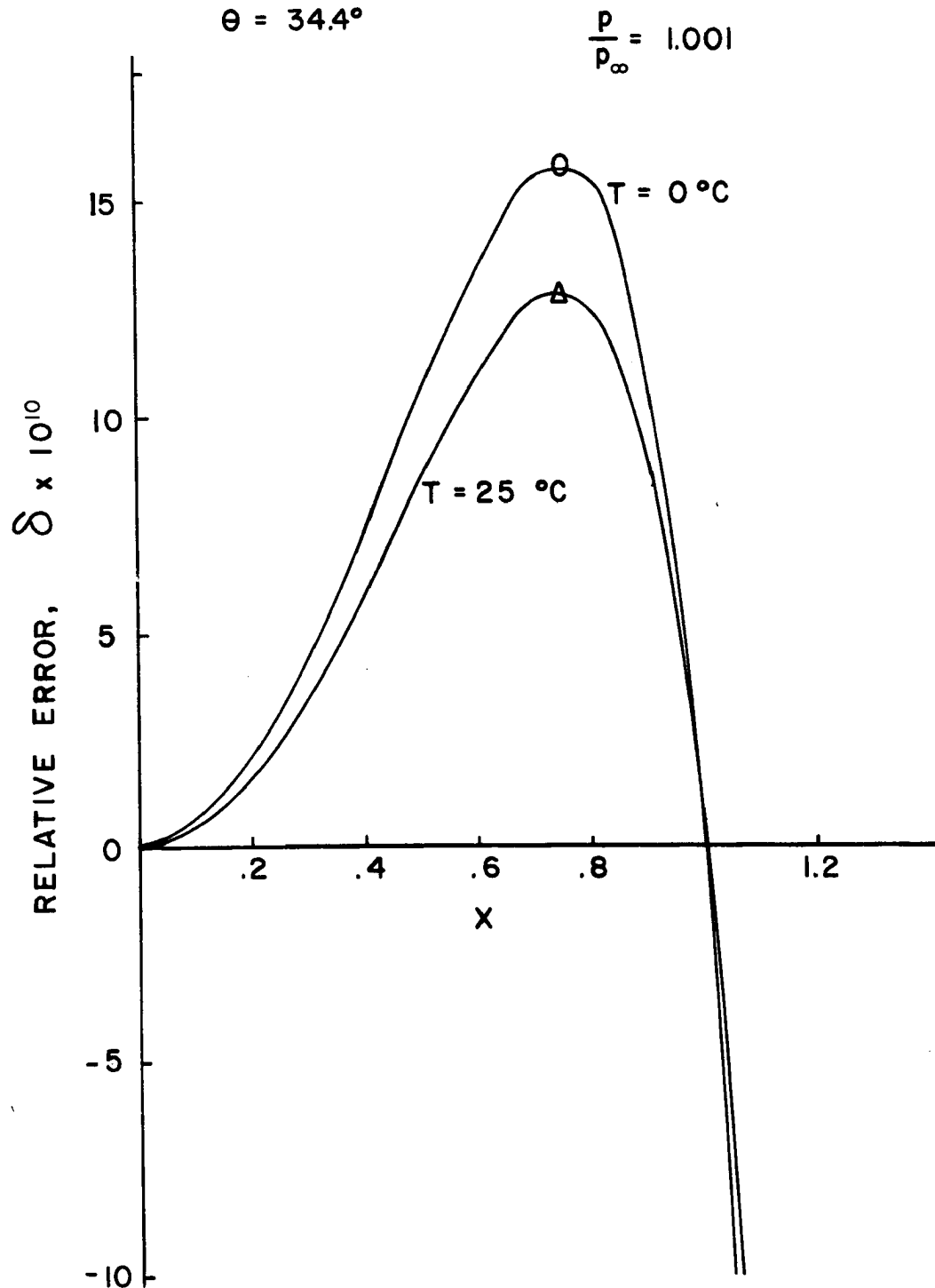


Figure 4. The relative error in assuming $\Delta G_{\text{sessile drop}}$ is given by $\Delta G_{\text{spherical cap}}$ for 0.1 percent supersaturation and a contact angle of 34.4 degrees as a function of \underline{X}

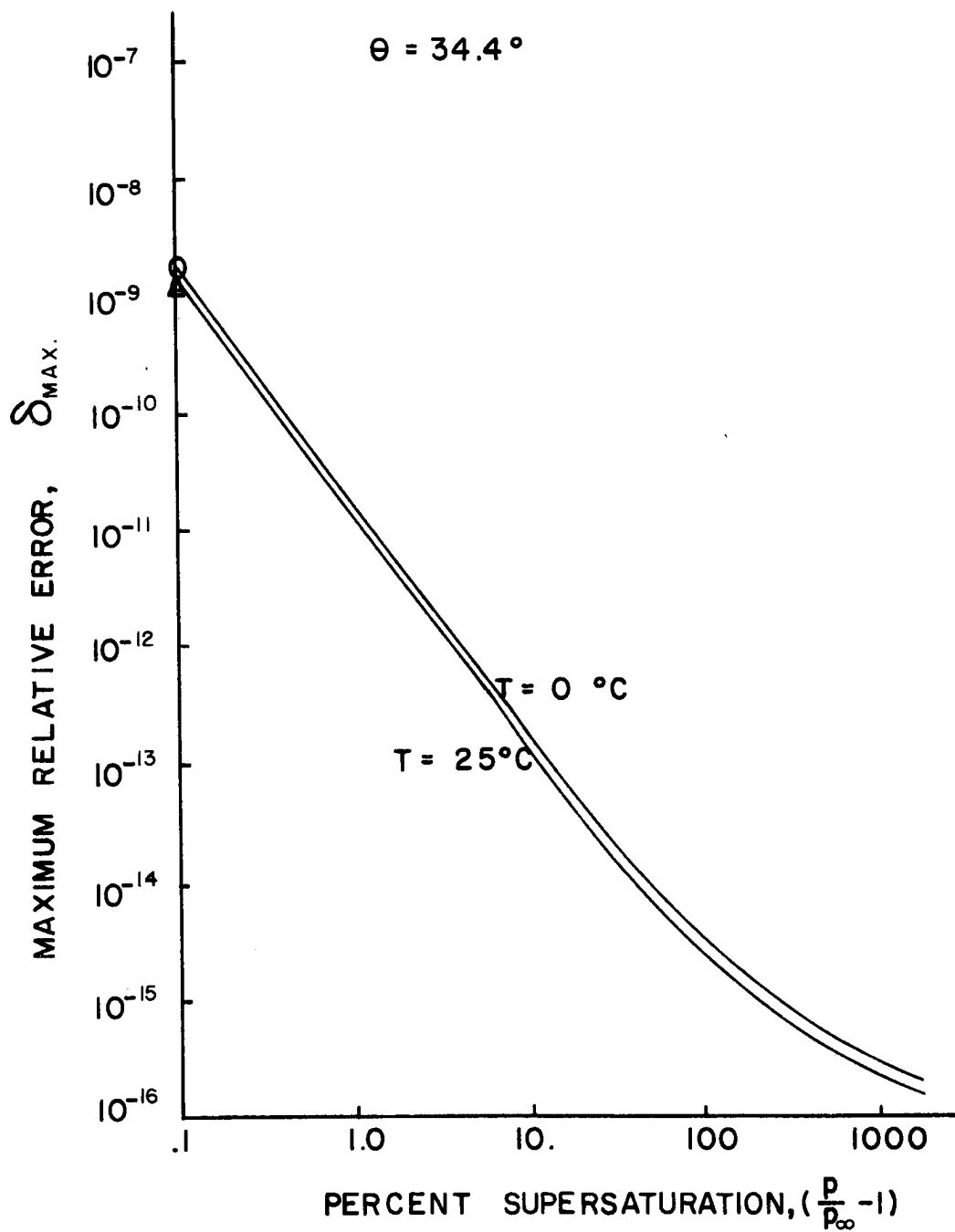


Figure 5. The maximum relative error as a function of the supersaturation at a contact angle of 34.4 degrees

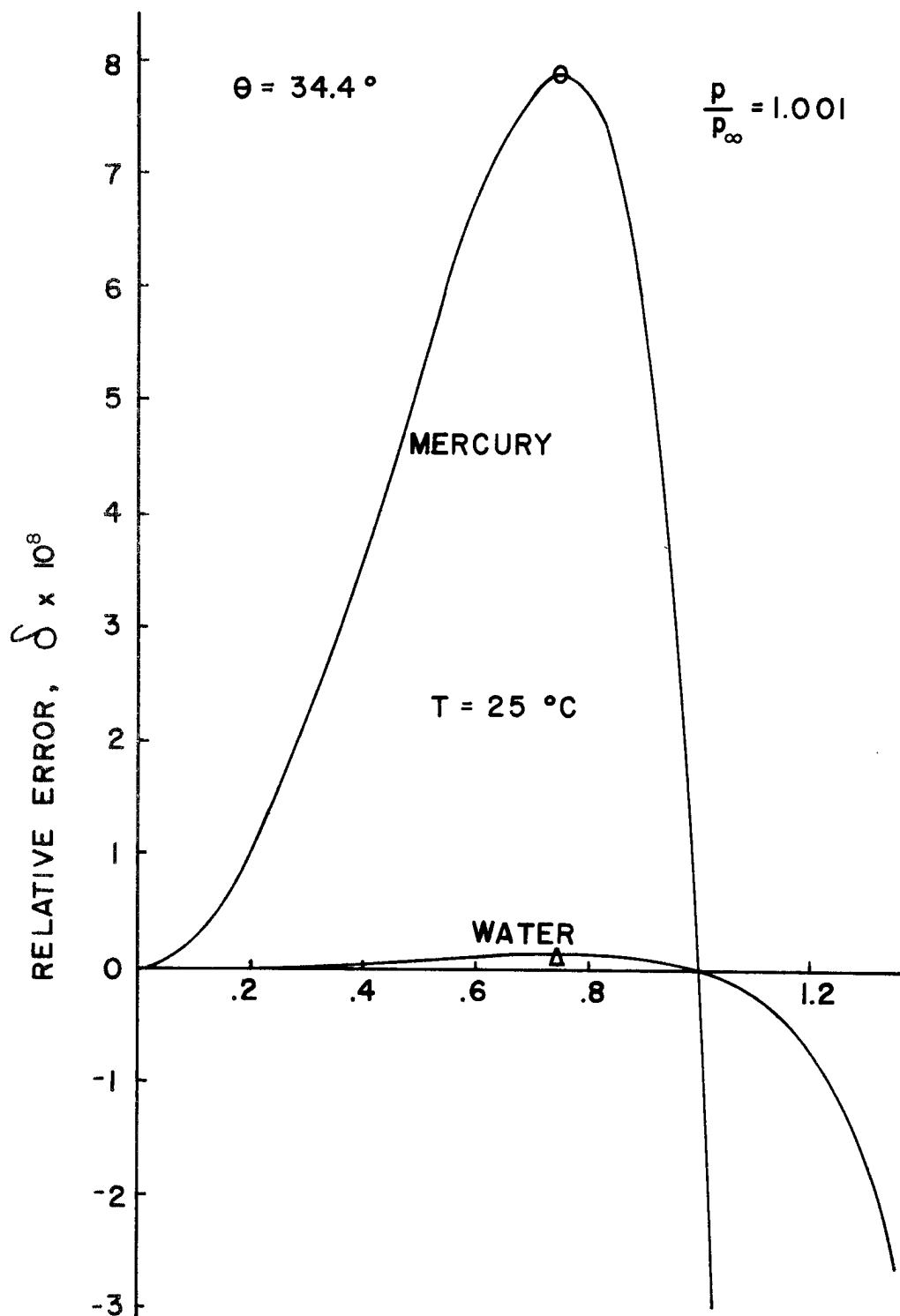


Figure 9. The relative error for mercury compared to water at a supersaturation of 0.1 percent and contact angle of 34.4 degrees as a function of X

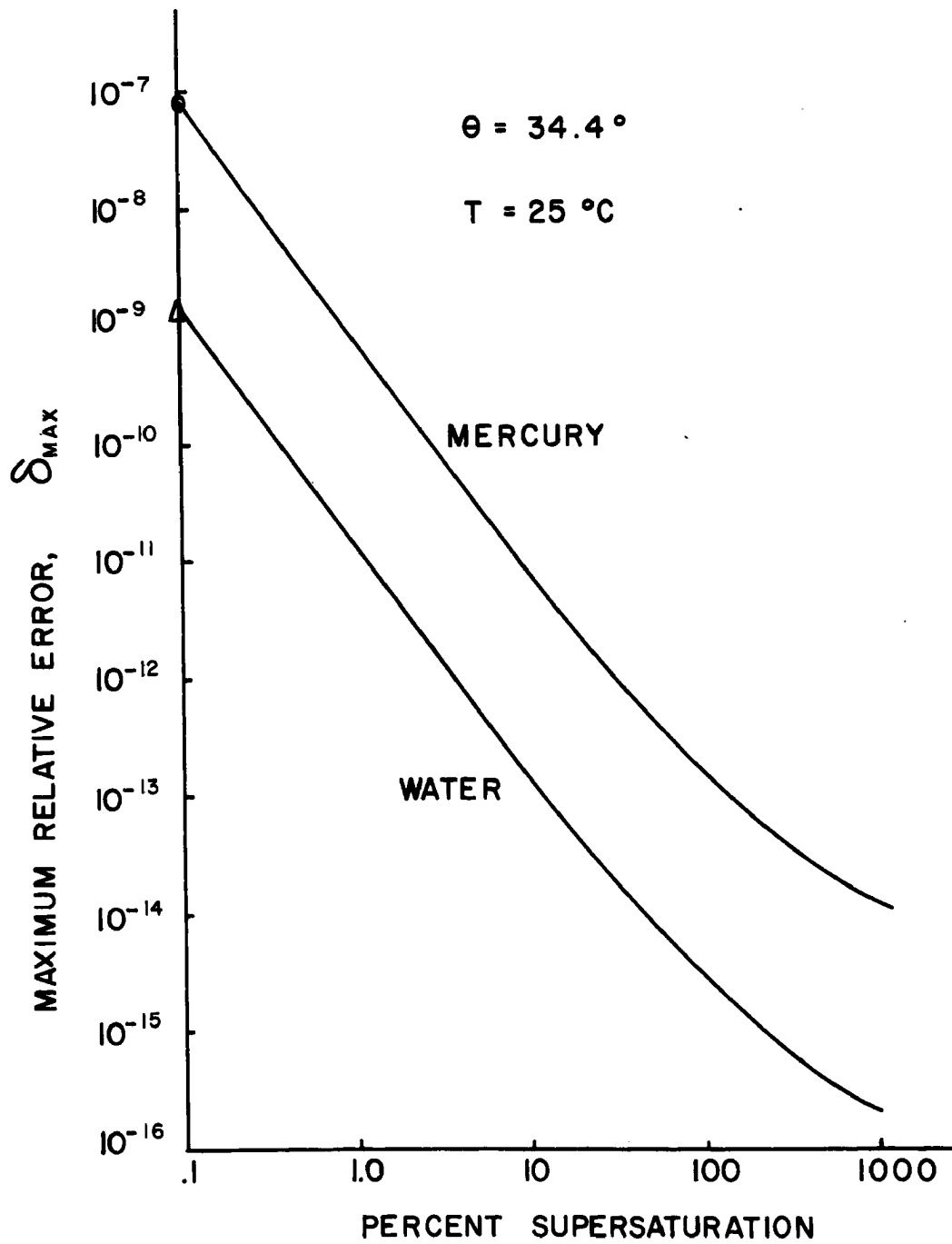


Figure 10. The maximum relative error for mercury compared to that for water as a function of supersaturation at a contact angle of 34.4 degrees

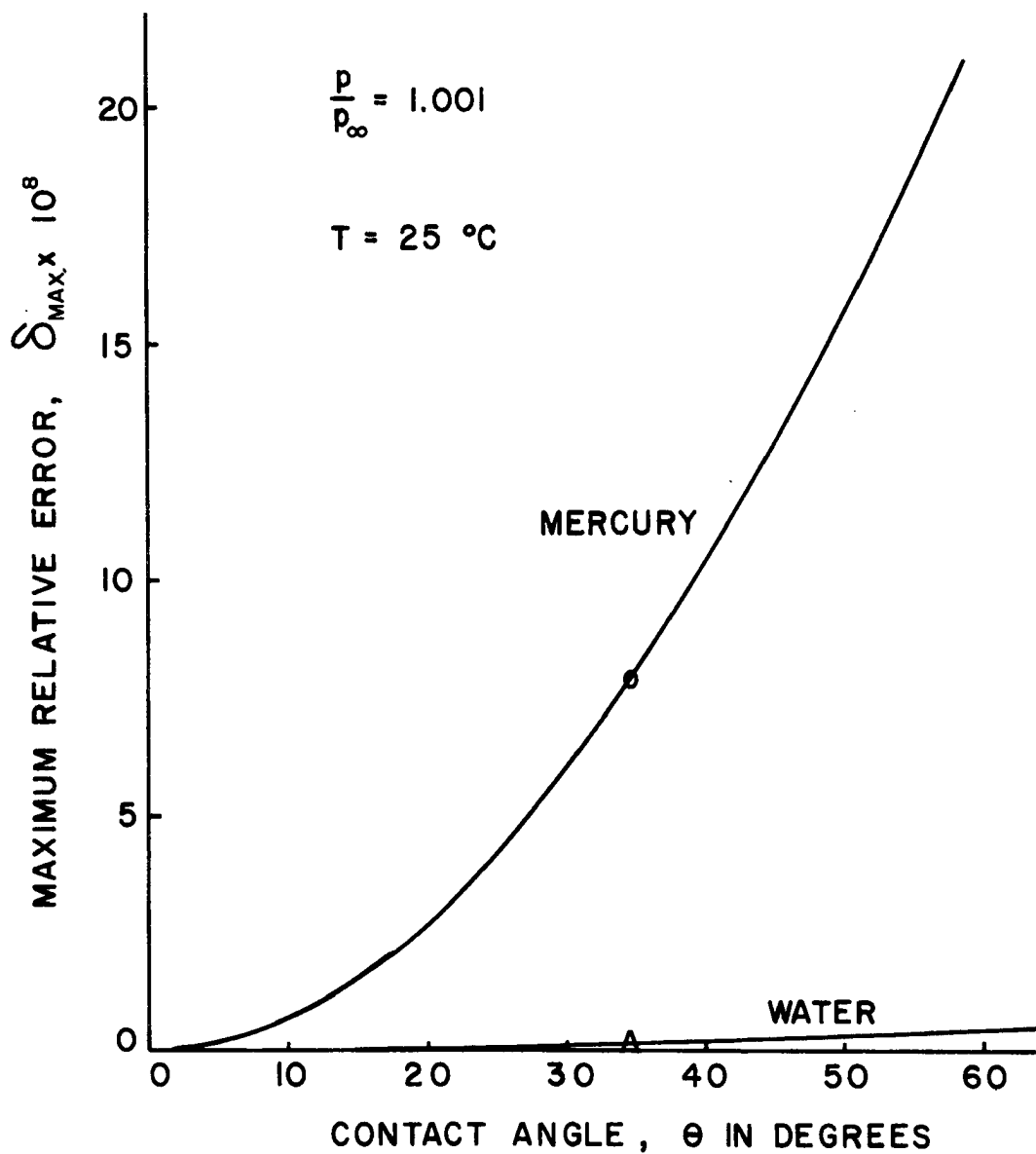


Figure 11. The maximum relative error for mercury compared to that for water as a function of the contact angle at a supersaturation of 0.1 percent

CONCLUDING REMARKS

A direct application of thermodynamics to the nucleation of a condensed phase leads to free energy change equations that are not based on a specific embryo geometry. Spherical approximation to the shape of the embryo results in the equations generally seen in texts on nucleation. In such texts, however, the problem of nonspherical embryos is generally avoided. A conclusion based on equation 16 is that for homogeneous nucleation a spherical embryo has the lowest free energy change of formation.

The effect of a nonspherical embryo on heterogeneous nucleation is investigated using a sessile drop as the embryo. Series equations describing the volume and surface areas of the sessile drop are derived. These equations are then substituted into the general free energy equation. The result is that the free energy change of the system for the formation of a sessile drop embryo can be expressed as the free energy change of the system for the formation of a spherical cap embryo plus a small correction term. Because the correction term is small, an expression for the relative error is also derived. The behavior of these two errors is investigated for maxima, zeros, and dependence on physical parameters. From equations 52 and 53 a general set of comparison ratios can be derived that allow a comparison of errors for different

systems or sets of parameters;

$$\frac{\Delta_1}{\Delta_2} = \left(\frac{d_2}{d_1}\right)^3 \left(\frac{M_1}{M_2} \frac{\sigma_{L, V_1}}{\sigma_{L, V_2}} \frac{T_2}{T_1} \frac{\ln(p/p_\infty)_2}{\ln(p/p_\infty)_1}\right)^4 \left(\frac{\theta_1}{\theta_2}\right)^6 \quad (58)$$

$$\frac{\delta_1}{\delta_2} = \frac{d_2}{d_1} \frac{\sigma_{L, V_1}}{\sigma_{L, V_2}} \left(\frac{M_1}{M_2} \frac{T_2}{T_1} \frac{\ln(p/p_\infty)_2}{\ln(p/p_\infty)_1}\right)^2 \frac{f(\theta_2)}{f(\theta_1)} \left(\frac{\theta_1}{\theta_2}\right)^6 \quad (59)$$

These ratios are valid only if \underline{x} is much different from unity and taken to be the same value in each system. With equations 58 and 59 it is possible to evaluate the errors for any system or conditions if the values of the error are known for one set of data. By using the following hypothetical data a set of errors is computed and presented in figures 12 and 13:

$$T = 1, \quad \sigma_{L, V} = 1, \quad \ln(p/p_\infty) = 1, \quad M = 1, \quad d = 1, \quad \theta = 1.$$

Values of the error presented in these figures as a function of \underline{x} can be used along with equations 58 and 59 to give the errors for any real system (except near the critical radius).

The magnitude of the error for real systems discussed in the last section and presented in figures 3 to 11 indicates that these errors are negligible from an experimental view point. A relative error of 10^{-7} , the maximum relative error for mercury, is probably beyond the limit of detectability. At the critical radius the relative error is several orders of magnitude smaller than the

maximum error. These results, therefore dispell the uncertainty of using the spherical cap model in heterogeneous nucleation on a plane, horizontal surface. While only computations for the sessile drop are made, it seems reasonable to extend this general conclusion to other shapes such as pendent drops or drops on non-horizontal surfaces. However, as pointed out by Fletcher (1962) and Turnbull (1950) nonplanar surfaces have a large influence on the energetics of nucleation.

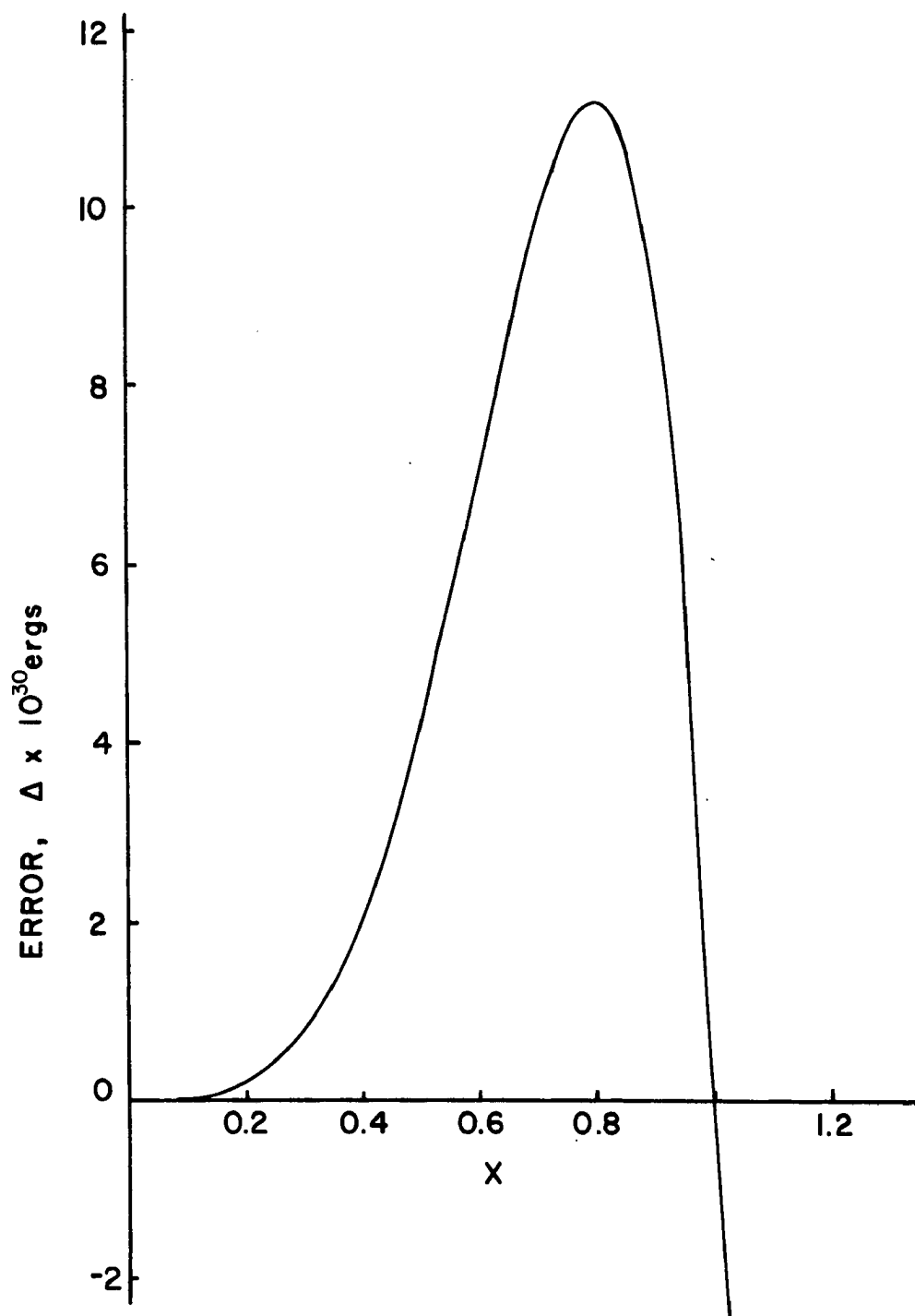


Figure 12. The error in assuming $\Delta G_{\text{sessile drop}}$ is given by $\Delta G_{\text{spherical cap}}$ for the hypothetical case as a function of X

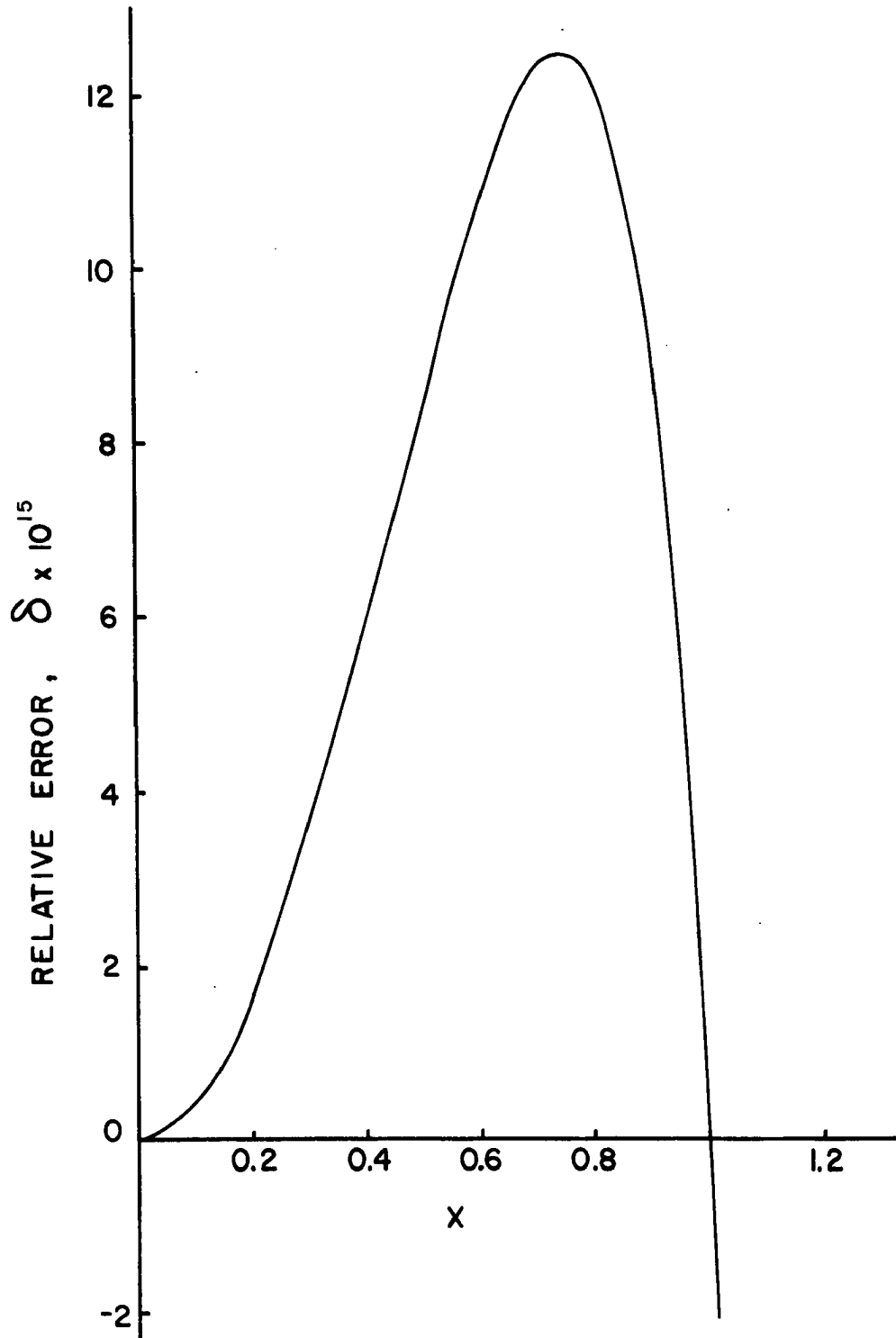


Figure 13. The relative error for the hypothetical case as a function of \underline{X}

BIBLIOGRAPHY

- Adamson, A. W., 1960: Physical Chemistry of Surfaces, Interscience, 747 pp.
- _____, and I. Ling, 1964: The Status of Contact Angle as a Thermodynamic Property, Contact Angle, Advances in Chemistry Series 43, American Chemical Society, Allied Publications, pp. 57-73.
- Bashforth, F., and J. C. Adams, 1883: An Attempt to Test the Theories of Capillary Action, Cambridge University Press, 80 pp.
- Fletcher, N. H., 1962: The Physics of Rainclouds, Cambridge University Press, chapter 3.
- Frenkel, J., 1939: A General Theory of Heterophase Fluctuations and Pretransition Phenomena, J. of Chem. Phys., 7, pp. 538-47.
- _____, 1946: Kinetic Theory of Liquids, Oxford University Press, pp. 366-90.
- Gibbs, J. W., 1906: Equilibrium of Heterogeneous Substances, The Scientific Papers of J. Willard Gibbs, Ph. D., LL. D., Vol. 1, Longmans, Green and Co., pp. 219-58.
- Gould, R. F., ed., 1964: Contact Angle, Advances in Chemistry Series 43, American Chemical Society, Allied Publications, 379 pp.
- Guggenheim, E. A., 1949: Thermodynamics (1st edition), North Holland Publishing Co., chapter 1.
- LaMer, V. K., and G. M. Pound, 1949: Surface Tension of Small Droplets from Volmer and Flood's Nucleation Data, J. of Chem. Phys., 17, pp. 1337-1338.
- Michaels, A. S., 1966: Nucleation Phenomena, American Chemical Society Publications, 85 pp.

- Tolman, R. C., 1948: Consideration of the Gibbs Theory of Surface Tension, J. of Chem. Phys., 16, pp. 758-74.
- _____, 1949: The Effect of Drop Size on Surface Tension, J. of Chem. Phys., 17, pp. 333-337.
- Turnbull, D., and J. C. Fisher, 1949: Rate of Nucleation in Condensed Systems, J. Chem Phys., 17, pp. 71-73.
- _____, 1950: Kinetics of Heterogeneous Nucleation, J. of Chem. Phys., 18, pp. 198-203.
- Uhlman, D. R., and B. Chalmers, 1966: The Energetics of Nucleation, Nucleation Phenomena, American Chemical Society Publications, pp. 1-13.
- Volmer, M., 1939: Kinetik der Phasenbildung, Steinkopff, p. 100, cited by N. H. Fletcher, 1962: The Physics of Rainclouds, Cambridge University Press, chapter 3.
- _____, and A. Weber, 1926: Keimbildung in übersättigen Gebilden, Z. Phys. Chem., 119, p. 277, cited by N.H. Fletcher, 1962: The Physics of Rainclouds, Cambridge University Press, chapter 3.

APPENDIX I

SERIES SOLUTIONS FOR SESSILE DROP SHAPE

Series solutions to the equations describing the sessile drop developed by Bashforth and Adams (1883) are based on the following equations

$$\frac{1}{\rho} + \frac{\sin \phi}{x} = 2 + \beta z \quad (\text{I-1})$$

$$dx = \rho \cos \phi dz \quad (\text{I-2})$$

$$dz = \rho \cos \phi dz . \quad (\text{I-3})$$

A series solution to ρ is assumed to be of the form

$$\rho = 1 + b_2 \phi^2 + b_4 \phi^4 + b_6 \phi^6 + \dots . \quad (\text{I-4})$$

Using the series expansions for $\sin \phi$ and $\cos \phi$ equations I-2 and I-3 can be integrated to give x and z as power series in ϕ . The coefficients of the powers of ϕ are functions of b_2, b_4, b_6, \dots , etc. By generating the inverse of ρ and $\sin \phi/x$ as power series, equation I-1 is used to obtain expressions for b_2, b_4, b_6, \dots , etc. in terms of β

Substituting for the coefficients of ϕ found for the variables x, z, ρ , and $1/\rho$ results in the following series in ϕ and β

$$\left(\frac{233}{14515200} \beta - \frac{17}{725760} \beta^2 + \frac{1517}{2211840} \beta^3 + \frac{7409}{2764800} \beta^4 + \frac{522091}{88473600} \beta^5 \right) \phi^{10}$$

(I-8)

The coefficients of the powers of $\underline{\phi}$ are exact. These series solutions give the exact value of the variables \underline{x} , \underline{z} , $\underline{\rho}$, and $\underline{1/\rho}$ provided that $\underline{\beta}$ and $\underline{\phi}$ are small so that the series converge.

APPENDIX II

COMPUTER PROGRAM

The data for the curves in figures 3 to 13 were computed by using the modified Fortran IV program presented in figure 14 on the CDC 6400 computer at Colorado State University. This program was a simplification of the program used to generate most of the data and was modified by removing DO loops that previously incremented the values of supersaturation and contact angle.

Numerical values printed by the computer include the free energy change of the system for the formation of both the spherical cap and sessile drop embryo, the error Δ , the relative error δ , and the critical radius of the spherical cap embryo. The error and relative error were computed from equations 42 and 48, respectively. The free energy change for the sessile drop case was computed as in equation 41.

Only four significant figures were used in the output since the magnitude of the error was much smaller than the free energy changes and could have only been detected by using double precision computations. A larger number of significant figures would not have added appreciably to the value of this study.

```

PROGRAM DFEC
C PROGRAM DFEC COMPUTES THE FREE ENERGY CHANGE OF THE SYSTEM FOR THE
C FORMATION OF A SPHERICAL CAP AND SESSILE DROP EMBRYO AND COMPARES
C THE DIFFERENCE BETWEEN THE TWO VALUES. BOTH THE ERROR AND RELATIVE
C ERROR ARE COMPUTED
DIMENSION A(4),C(3)
50 FORMAT(1H1,14HSURFACE TENSION=,F7.3,10X, 8HDENSITY=,F8.4,10X,
1 13HMOLAR VOLUME=,F7.3/)
100 FORMAT(1H ,2X,3HPHI,5X,1HT,5X,3HSSR,7X,2HRC,10X,2HGRC,13X,1HB,10X,
1 2HGS,10X,2HGD,9X,9HGS-GD,4X,10H(GS-GD)/GS)
200 FORMAT(1H ,F5.1,2X,F5.0,2X,F6.3,2X,E10,3,2X,F10,3)
300 FORMAT(1H ,46X,6(2X,E10,3))
C R IS THE GAS CONSTANT
R=8.31696E+7
C G IS THE GRAVITATIONAL CONSTANT
G=980.
C ST IS THE SURFACE TENSION
D=1.
C D IS THE DENSITY OF THE LIQUID PHASE
ST=1.
C WM IS THE MOLECULAR WEIGHT
WM=1.
C T IS THE TEMPERATURE IN DEGREES KELVIN
T=1.
C VM IS THE MOLAR VOLUME OF THE CONDENSED PHASE
VM=WM/D
WRITE(6,50) ST,D,VM
WRITE(6,100)
PI=3.1415927
C PHI IS THE CONTACT ANGLE IN RADIANS
PHI=1.
C ANG IS THE CONTACT ANGLE IN DEGREES OF ARC
ANG =180.*PHI/PI
CA=COS(PHI)
C F IS THE FLETCHER FORM FACTOR MODIFYING THE FREE ENERGY CHANGE
F=PI*(2.+CA)*(1.-CA)**2)
C SSR IS THE SUPERSATURATION RATIO FOR A GIVEN TEMPERATURE T
SSR=2.718281828
C SS IS THE KELVIN FACTOR
SS=-T*R*ALOG(SSR)/VM
C RC IS THE CRITICAL RADIUS OF THE SPHERICAL CAP EMBRYO
RC=-2.*ST/SS
DR=RC/20.
RD=DR
C GC IS THE CRITICAL FREE ENERGY CHANGE FOR THE SPHERICAL CAP
GC=(SS*(RC**3)/3. + ST*RC*RC)*PI*F
WRITE(6,200) ANG,T,SSR,RC,GC
DO 1 I=2,6,2
→ 1 A(I)=PHI**I
DO 20 I=1,30
C R IS THE RADIUS OF CURVATURE AT THE VERTEX OF THE SESSILE DROP
H=DR*(I-1)+RD
C GS IS THE FREE ENERGY CHANGE FOR THE SPHERICAL CAP EMBRYO
GS=(SS*H*R*R/3. + ST*R*B)*PI*F
C RFTA IS THE SHAPE PARAMETER FOR THE SESSILE DROP
HETA=G*RD*R*R/ST
C(1)=RFTA
C(2)=C(1)*C(1)
C(3)=C(1)*C(2)
C DEL IS THE ERROR IN ASSUMING THE SESSILE DROP TO BE A SPHERICAL CAP
DEL= PI*G*DA(6)*(H**4) *(1.-R/RC)*(5./24.-(3./32.+
1133.*C(1)/1536.)*A(2)+(23./1152.+107.*C(1)/5760.+217.*C(2)/5120.)*
2 A(4)-(479./181440.+2189.*C(1)/18432.+3581.*C(2)/138240.+33473.*
3 C(3)/1474560.)*A(6)+C(1)*A(2)*(3/RC)*(7./512.-(31./3840.+27.*
4 C(1)/2560.)*A(2)+(301./13824.+133.*C(1)/18432.+3091.*C(2)/
5 442368.)*A(4)))
C DDG IS THE RELATIVE ERROR MADE BY ASSUMING THE SESSILE DROP
C TO BE A SPHERICAL CAP
IF(I,LT,30) DDG=DEL/GS
C DG IS THE FREE ENERGY CHANGE FOR THE SESSILE DROP
DG=GS-DEL
WRITE(6,300) R,GS,DG,DEL,DDG
20 CONTINUE
END

```

Figure 14. The computer program for computing the free energy change

APPENDIX III
TABULATED DATA

A summary of the numerical computations involved in producing figures 3 to 13 is given in the following tables. Table 1 gives the values of the physical parameters used as input data to the computer program presented in Appendix II.

Table 2 summarizes the variation of the errors, $\underline{\Delta}$ and $\underline{\delta}$, as a function of \underline{x} . The units of the error, $\underline{\Delta}$, are ergs, while $\underline{\delta}$ is nondimensional.

Table 3 summarizes the variation of the maximum relative error, $\underline{\delta}_{\max}$ and the relative error at the critical radius, $\underline{\delta}_{r^*}$, as a function of the supersaturation at a constant contact angle of 34.4 degrees.

Table 4 summarizes the variation of the maximum relative error and the relative error at the critical radius as a function of the contact angle at a constant supersaturation of 0.1 percent.

TABLE 1
INPUT DATA

	T	$\sigma_{L, V}$	d	M	θ	p/p ∞
	$^{\circ}\text{K}$	erg/cm 2	gm/cm 3	gm/mole	degrees	
WATER	273	74.92	0.9970	18.0	11.5	1.001
	298	71.97	0.99987	18.0	to	to
MERCURY	298	484.	13.534	200.61	57.3	11.00
HYPOTHETICAL	1	1.	1.	1.	57.3	2.718

TABLE 2
THE ERROR AND RELATIVE ERROR
AS A FUNCTION OF \underline{X}

X	$\theta = 34.4^\circ$		$(p/p_\infty - 1) \times 100 = 0.1$			HYPOTHETICAL	
	T = 0 °C		T = 25 °C				
	WATER		WATER		MERCURY		
	$\Delta \times 10^{17}$	$\delta \times 10^{10}$	$\Delta \times 10^{17}$	$\delta \times 10^{10}$	$\Delta \times 10^8$	$\Delta \times 10^{30}$	$\delta \times 10^{15}$
0.10	0.03	0.44	0.05	0.54	0.27	0.01	0.43
0.20	0.39	1.68	0.65	2.08	1.04	0.17	1.64
0.30	1.74	3.59	2.88	4.44	2.21	0.77	3.49
0.40	4.72	5.97	7.80	7.38	3.67	2.09	5.80
0.50	9.60	8.54	15.90	10.57	5.26	4.24	8.31
0.60	15.92	10.89	26.31	13.53	6.73	7.04	10.64
0.70	22.12	12.56	36.56	15.54	7.73	9.78	12.22
0.75	24.29	12.82	40.15	15.85	7.88	10.74	12.47
0.80	25.16	12.50	41.58	15.46	7.69	11.13	12.16
0.85	24.04	11.40	39.74	14.10	7.01	10.63	11.09
0.90	20.15	9.23	33.30	11.41	5.68	8.91	8.98
0.95	12.51	5.61	20.67	6.94	3.45	5.53	5.46
1.05	-18.66	-8.37	-30.85	-10.36	-5.15	-8.25	-8.14
1.10	-44.96	-20.68	-74.31	-25.58	-12.72	-19.88	-20.11
1.15	-80.56	-38.75	-	-47.92	-23.83	-35.63	-37.68

TABLE 3
DEPENDENCE OF THE RELATIVE ERROR
ON THE SUPERSATURATION

	$\theta = 34.4^\circ$				
	$T = 0^\circ\text{C}$		$T = 25^\circ\text{C}$		
	WATER		WATER		MERCURY
	$X = 0.75$	$X = 1.0$	$X = 0.75$	$X = 1.0$	$X = 0.75$
$(p/p_\infty - 1) \times 100$	δ_{\max}	δ_{r^*}	δ_{\max}	δ_{r^*}	δ_{\max}
0.1	1.585×10^{-9}	8.633×10^{-17}	1.282×10^{-9}	5.644×10^{-17}	7.885×10^{-8}
1.0	1.600×10^{-11}	8.790×10^{-21}	1.293×10^{-11}	5.747×10^{-21}	7.956×10^{-10}
10.	1.743×10^{-13}	1.057×10^{-24}	1.410×10^{-13}	6.932×10^{-25}	8.671×10^{-12}
100.	3.296×10^{-15}	6.231×10^{-28}	2.665×10^{-15}	6.480×10^{-28}	1.639×10^{-13}
1000.	2.754×10^{-16}	2.348×10^{-29}	2.227×10^{-16}	1.858×10^{-29}	1.622×10^{-14}